

3.3 Structure Model Analysis of the Kashima 34m Telescope

By

Junichi NAKAJIMA, Takeshi SAITA, Junji HORIGUCHI, and Kouhei YUGE

ABSTRACT

Deformation analysis of the Kashima 34-m radio telescope is performed. Although the telescope has a large aperture and accurate reflector panels, the dish support structures determine the high frequency performance. Especially in millimeter wavelengths, deformations above 1 mm greatly affect telescope efficiency. We have modeled the 34-m telescope into elements and used the Finite Element Method (FEM) to simulate accurate telescope deformations. The results of our analysis were found to agree well with realistic deformation. Future analysis and telescope evaluations based on computer are possible with this FEM model.

Keywords: FEM (Finite Element Method), Antenna structural analysis

1. Overview

The Kashima 34-m radio telescope of the Communications Research Laboratory (CRL), the third largest radio telescope in Japan, was constructed in 1988 and began full operations in 1990. In the research described here, we use the finite element method (FEM) to model the 34-m parabola and confirm the validity of analysis. The need for this model arose from the difficulty involved in directly measuring deformation in the reflector surface from its ideal state at various angles of elevation, which in turn makes it difficult to determine the extent of degraded efficiency when usage frequency changes from microwaves to millimeter waves. Predictions made beforehand from mechanical deformation can therefore provide valuable information when deciding whether a receiver in higher frequency can be mounted. In addition, a model can be very useful in maintenance work by isolating those structural elements of an existing parabola subjected to the most stress, and can be used for studies of next-generation large parabolas. Although holographic methods using radio tones from satellites can now be used to measure deformation at specific elevation angles and determine intra-panel or inter-panel differences, estimating the degree of global deformation in the basic structure of the antenna is an essential first step. This is the first genuine application of FEM to the Kashima 34-m antenna.

2. Background to the Kashima 34-m Antenna and Overseas Developments

Design of the Kashima 34-m antenna is originated in the 1980's as an extension of general 32-m INERSAT communications parabolas, and the antenna eventually became a special multi-frequency design of antennas used in the Deep Space Network (DSN) of the National Aeronautics and Space Administration (NASA). An even older 34-m antenna of this type was the NASA DSS-15 (where "15" is a NASA sequence number; see Fig. 1) constructed in 1984 by TIW Systems. This antenna together with similar antennas in Canberra, Australia and

Madrid, Spain made history by receiving images from the Voyager deep-space probe during its flyby of Uranus. The telescope structure manufacturer, TIW Systems, confirmed that efficiency was maintained and that sufficient performance was achieved for deep space links on NASA-DSN at a wavelength of 37.5 mm (8 GHz). On the basis of these results, we decided to give the Kashima 34-m an-



Fig. 1 The NASA DSS-15 antenna in Goldstone, California similar in design to the Kashima 34-m antenna

This antenna is equipped with only 2- and 8-GHz receivers and its some of the large panels have been converted into mesh.

tenna high-accuracy panels with a rms-value of 0.17 mm that can support wavelengths as far as the millimeter level. We also maintained a maximum drive speed of 1° /sec from the lightweight structure despite the large size of the antenna and thereby achieved a level of performance suitable for geodetic VLBI observations. With regard to structure, however, the Kashima 34-m antenna is a parabola that uses relatively thin-walled materials and that has not been optimized for millimeter-wave targets. For these reasons, we recognize the need for prior studies by an FEM model to determine the extent to which gravitational deformation, wind-induced deformation, and other forms of deformation might occur. Without such information, not only it is impossible to explain the observation performance, it also be impossible to make accurate evaluations even when observing astronomical targets.

Overseas, large telescope projects are now moving forward in a number of countries. For example, construction of the Greenbank Telescope, which will be the world's largest steerable telescope, is now in progress, and other next-generation large-telescope projects are underway in Europe (Bologna University), Australia (Square Kilometer Array (SKA)), and elsewhere. Many of these projects are pursuing large-telescope models applicable to computational mechanics.

3. Finite Element Method

The finite element method in structural analysis divides the target structure into finite elements, represents those elements in the form of approximate simultaneous first-order equations, and mathematically solves for elas-

tic deformation in the elements. The nodes that connect the elements define the shape of these elements. Here, by determining for each element an element synthesis matrix that defines node-to-node strain relationships and then combining corresponding sections, a formulated matrix for the entire structure can be prepared. If this matrix can then be solved after giving appropriate constraints based on a realistic model, displacement of the structure when a force is applied can be determined. Statically, displacement δ can be determined from stiffness matrix K and external force F as follows.

$$K \cdot \delta = F$$

$$\delta = K^{-1} \cdot F$$

In the FEM-based analysis described here, we used general-purpose finite-element modeling software and FEMAP/ANSYS analysis software currently being used at the Department of Mechanical Engineering, Faculty of Engineering, of Seikei University⁽²⁾.

4. Modeling of the Kashima 34-m Antenna

On modeling the Kashima 34-m antenna shown in Fig. 2, we measured all members in the main-reflector support section and used these to form an element model. Figure 3, 4, and 5 show the 34-m antenna model created by computer. Comparing this model with the actual antenna structure, we specified constraints on the nodes and determined deformation when applying gravitational acceleration as shown in Fig. 6. In this model, the structural material of the antenna is assumed to be steel, and for a Young's modulus of 2.06×10^{11} , a Poisson ratio of 0.3, and a density of 7836.7 kg/m^3 , the total weight of

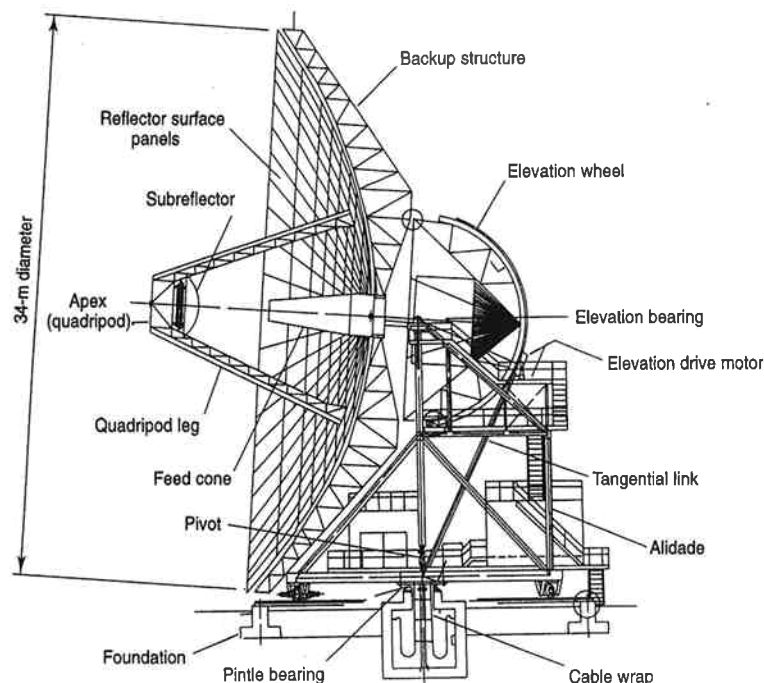


Fig. 2 Basic structure of the Kashima 34-m antenna

The panels of the main reflector are supported by a framework called a "backup structure". This structure rotates about the elevation axis and is balanced by a counterweight on the other side (see Ref. 1)

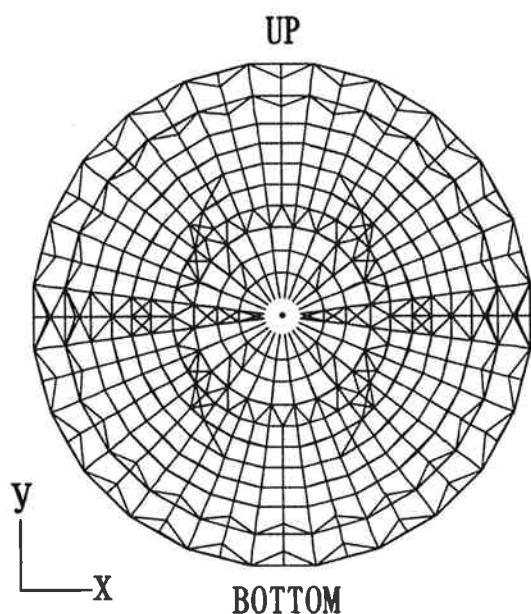


Fig. 3 34-m antenna FEM model

The radially directed truss and the circular hoop structure. Added structure for easing gravitational stress are be seen.

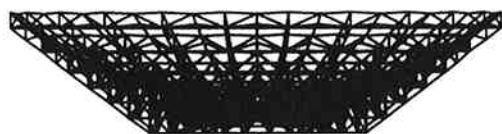


Fig. 4 34-m antenna FEM model

Outward appearance when viewed from the side resembles actual antenna.

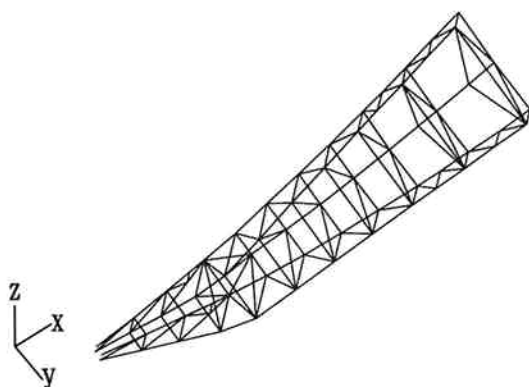


Fig. 5 1/24 model

Axially symmetric structure is generated on the basis of this model.

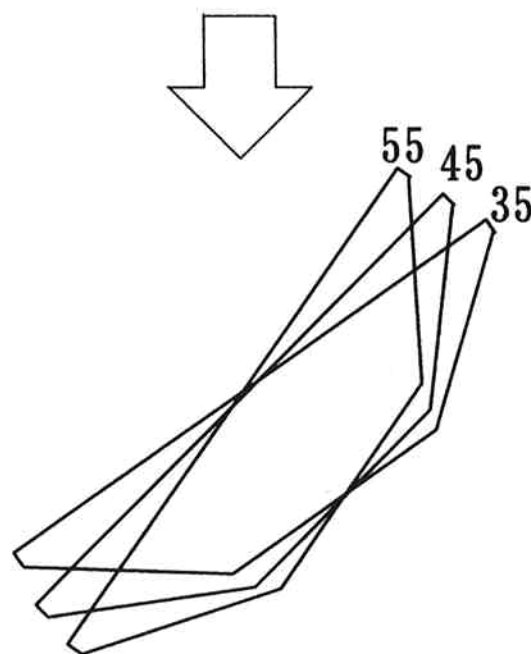


Fig. 6 Model orientation when applying gravitational acceleration

The gravitational acceleration vector is varied in the analysis.

these members was found to agree within several percent with the design weight specified by the antenna manufacturer. The cross sectional shapes were taken to be as shown in Table 1 and the structure of the 34-m antenna was modeled by combining ROD and TUBE elements. In this model structure, the base nodes are constrained by the center-hub section and the high-stiffness octagon-shaped pedestal that extends as one body from the EL axis. Panel mass was also added to perform deformation analysis. At first, we used only ROD elements and analyzed the 34-m antenna assuming a truss structure and pin support junctions. The results of this analysis indicated the occurrence of global deformation that took the form of significant constriction at contact points of the structural material within the hoop. In actuality, however, no such physical phenomenon was occurring. As a result of studying this problem, we decided to use rigidly connected ROD and TUBE elements for the entire radially directed truss within this section and proceeded with model analysis assuming a rigid frame. Eventually, we modeled the structure with BEAM elements that give more accurate cross-sectional 2nd-order moments, but both models provided nearly the same deformation results. The cross-sectional shapes and cross-sectional 2nd-order moments of BEAM elements (steel angular pipes) configuring the 34-m antenna as determined from measurement and calculation are given in Table 1. The following section presents the results of model analysis focusing mainly on the results of calculations by an FEM model using BEAM elements.

Table 1 Examples of shapes and calculated cross-sectional 2nd-order moments of angular pipes used in the 34-m antenna

Cross-sectional 2nd-order moments for twisting are also calculated in the model and reflected in the stiffness matrix.

| Size (height×width×thickness) [mm] | Cross-sectional Area [mm ²] | Cross-sectional 2nd-order Moment [m ⁴] |
|------------------------------------|---|--|
| 38.1×38.1×3.175 | 484 | 5.1614E - 08 |
| 50.8×50.8×3.175 | 645 | 1.2627E - 07 |
| 50.8×50.8×4.7625 | 967 | 1.8064E - 07 |
| 76.2×76.2×6.35 | 1935 | 8.2582E - 07 |
| 101.6×101.6×9.525 | 3871 | 2.8902E - 06 |
| 101.6×101.6×12.7 | 5161 | 3.6745E - 06 |
| 101.6×101.6×6.35 | 581 | 2.0203E - 06 |
| 101.6×101.6×4.7625 | 1934 | 1.5515E - 06 |
| 76.2×50.8×4.7625 | 1209 | 2.5159E - 07 |
| 101.6×101.6×7.9375 | 3222 | 2.4663E - 06 |
| 38.1×38.1×4.7625 | 725 | 7.2666E - 08 |

5. Model Analysis and Validity of Calculations

5.1 Method of evaluating a model conforming to an actual radio telescope

Deformation in the support structure of the 34-m telescope when adding panel loads is shown in Figs. 7 and 8. The upper and lower ends tend to drop for a given elevation angle. The maximum displacement shown by this deformation is at the lower end of the parabola at an absolute value of about 5 mm. On the actual antenna, panel surfaces can be adjusted within a range of ± 20 mm by bolts and nuts on pin support. At the time of antenna construction, a theodolite adjustment was used at night when thermal deformation is uniform to configure a parabola on a deformed structure in the elevation angle of 45° . This approach is different from that of polishing an ideal specular surface of an optical telescope. Accordingly, in evaluating deformation using a model, we also decided to investigate differences in deformation with that at an elevation angle of 45° used as a reference, the same as in an actual telescope. Deformation results for elevation angles of 55° and 35° are shown in Figs. 9 and 10, respectively. Maximum displacement at contours that extract deformation in the z direction, which affects focus distance, was found to be 0.8 mm. In addition, movement by the entire parabola downward can be seen to be 0.5 mm in Fig. 11. With parabola surface rms given by $\sigma = 1/4\pi$, this means a drop in gain of 37%, which is considered the limit in actual use. When applying this equation, a sufficient margin is given at 22 GHz (wavelength: 27 mm), but a significant drop in efficiency expected at 43 GHz (wavelength: 7 mm). Regions where these deformations occur, however, are sections where a taper is applied to radiation patterns from the sub-reflector in an optical

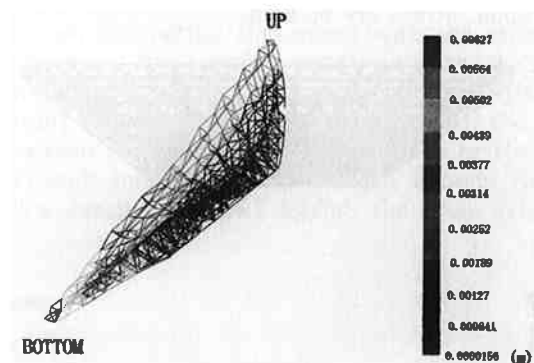


Fig. 7 Gravitational deformation in the 34-m structure for an elevation angle of 45°

The amount of deformation is emphasized for clarity, but it is only 0.6 mm at maximum, which is small relative to the size of the 34-m antenna; the desired parabolic shape is constructed on top of this deformation.

manner, which means that deformation effects are not fatal.

5.2 Peak of internal stress

Figures 12 and 13 show structure members where internal stress peaks. The value of stress including both tension and compression is about 16 MPa at maximum, and since this is sufficiently low compared to the elastic limit of 300 MPa, thus the deformation is elastic. Large tensile stress and compressive stress often exist side by side in the truss structure. It can be seen, however, that stress is widely dispersed in members along the EL axis due to nearby supplementary material that has been added to the axially symmetric structure.

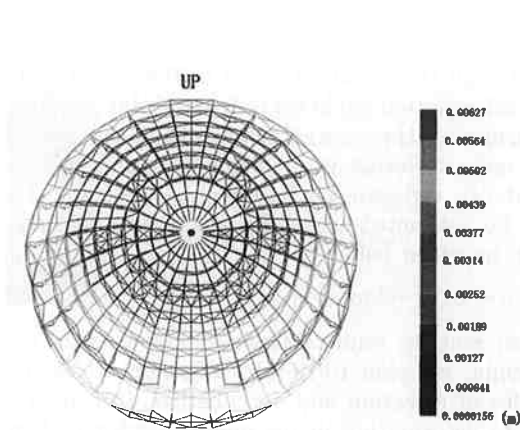


Fig. 8 Gravitational deformation in the 34-m structure for an elevation angle of 45°

In the elevation angle of 45° , the lower part structure shows a deformation of 0.6mm maximum. The amount of change is emphasized in the graphics.

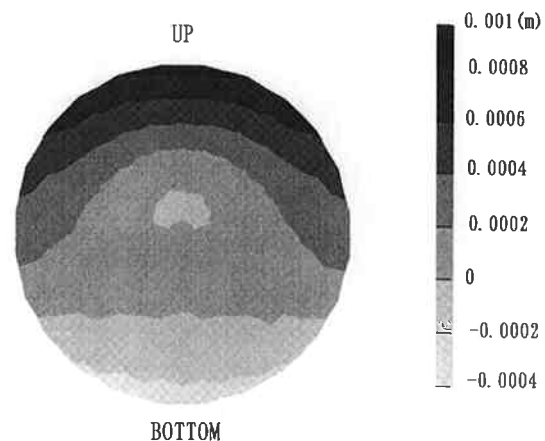


Fig. 10 Gravitational deformation in the 34-m structure in the direction of the z-axis for an elevation angle of 35°

Compared to an elevation angle of 45° , the upper and lower ends of the parabola show a displacement of about 1 mm from the ideal state; these results are symmetric to those at 55° .

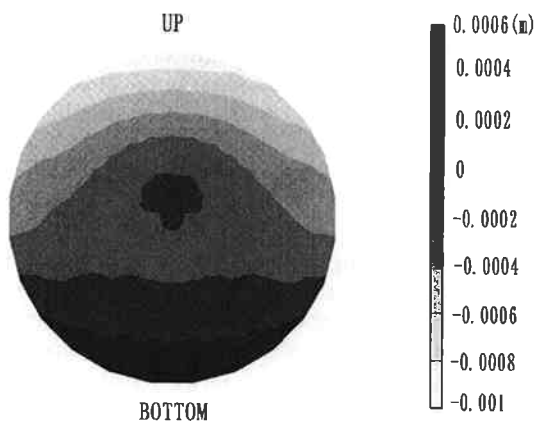


Fig. 9 Gravitational deformation in the 34-m structure in the direction of the z-axis for an elevation angle of 55°

Compared to an elevation angle of 45° , the upper and lower ends of the parabola show a displacement of about 1 mm from the ideal state.

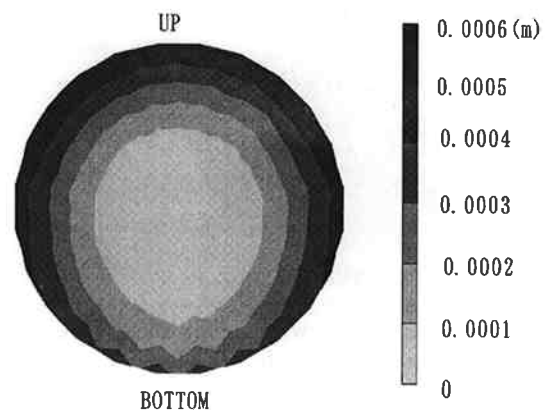


Fig. 11 Gravitational deformation in the 34-m structure in the direction of the xy-axes for an elevation angle of 35°

Compared to an elevation angle of 45° , the entire edge drops by about 0.5 mm.

5.3 Fluctuation in focus distance

Performance of a parabola antenna for operation at a certain frequency is usually represented as total performance of the cassegrain system including the shape of the main reflector, sub-reflector, and the feed system, or in other words, aperture efficiency η (ideally 1). In this study, however, we evaluated only the main reflector and calculated the displacement of each contact point from the ideal focus position. The results are shown in Fig. 14, and it can be seen that deformation is about 1 mm at maximum at an elevation angle of 35° . In this regard, there are large telescopes dedicated to millimeter-wave observations that are designed with a homologous structure in which the shape of the reflector can again be configured as a parabolic surface after deformation have

occurred. However, that this effect cannot be expected in the Kashima 34-m antenna. While it is possible that moving the sub-reflector can decrease the effects of deformation. From this mm-order deformation, the antenna efficiency will begin to drop in millimeter radio wave observations.

6. Summary and Future Issues

In this report, we have described the creation of finite elements for the Kashima 34-m antenna and the completion of a model that gives valid deformation results with regard to the actual antenna. In future research, we plan to pursue the following studies using this model.

(1) In the current study, we examined the validity of

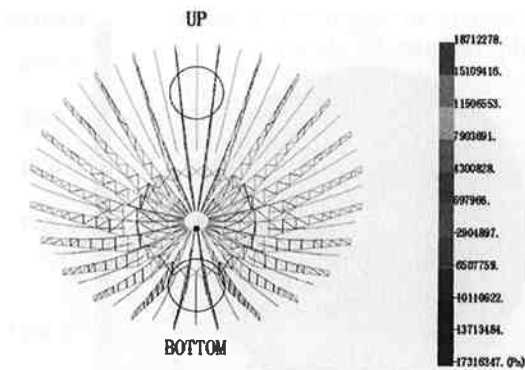


Fig. 12 Truss component where maximum stress occurs for an elevation angle of 35°
Tensile stress becomes maximum in the region marked by \bigcirc .

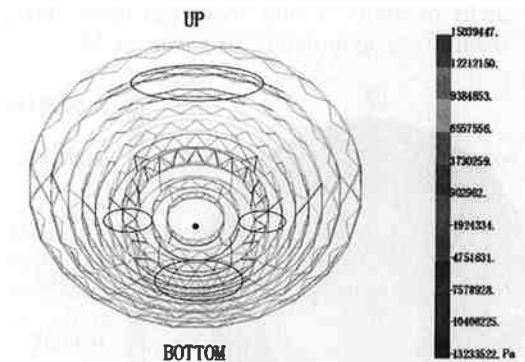


Fig. 13 Hoop component where maximum stress occurs for an elevation angle of 35°
Stress distribution becomes maximum in the region marked by \bigcirc .

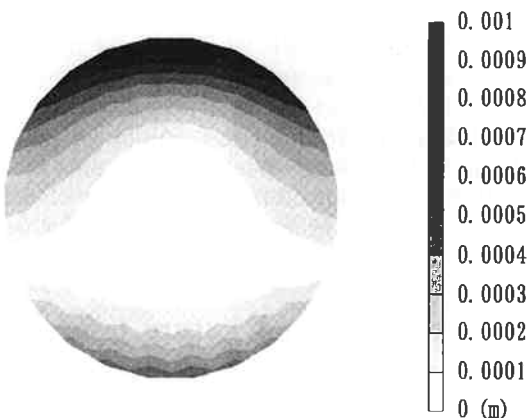


Fig. 14 Displacement converted to focus distance for an elevation angle of 35°
Compared to an elevation angle of 45° , the upper dish edge is already deformed by about 1 mm.

this model only at elevation angles of 35° and 55° centered about 45° due to time limitations. Our plan is to vary the elevation angle in the model and examine deformation at lower angles as far as 10° . After determining the rms value of surface deformation for the main reflector using panel rms and the displacement of reflector surface points, antenna efficiency can be estimated using Ruze's approximating equation, as given below⁽³⁾.

$$\eta = \exp[-4\pi\sigma/\lambda]^2$$

- (2) When making millimeter-wave observations with the antenna, we plan to obtain efficiency η for different angles of elevation and see whether drop in efficiency due to deformation in the main reflector is dominant. If other factors are found to contribute to a drop in efficiency, such as gravitational deformation in the support structure of the sub-reflector, these will likewise have to be modeled.
- (3) While it is impossible to make a daily check of all structural members that support the main reflector (they number over 2000), even more detailed tracking of changes in internal stress for individual elements will make it possible to specify locations that should receive attention during maintenance work. The study presented here revealed only those elements where maximum stress occurs, but it should be possible to extract elements that become twisted or experience large stress amplitudes while elevation angles change continuously, to check their welded points, etc.

Finally, establishing the model described in this report has provided a foundation for studies by computer simulations of next-generation large parabolic antennas. While the U.S. and Europe have radio telescopes of the 100-m class, Japan still has no large parabolic antennas more than 64 meters. Millimeter broadband frequency resources must be utilized in the future for performing data transmissions associated with deep space applications, and antennas for this purpose can now be studied by computer.

Acknowledgments

This research became possible with the cooperation of the Mechanical Design Laboratory in the Department Of Mechanical Engineering, Faculty of Engineering, of Seikei University. The author (Junichi Nakajima) would especially like to extend his deep appreciation to Professor Kouhei Yuge and Toshio Nakamura, Takeshi Saita, and Junji Horiguchi, for their valuable assistance.

References

- (1) Levy, R., "Structural Analysis of Microwave Antenna", 1996, IEEE Press.
- (2) Nakamura, T., "Analysis of Deformation by a Radio Telescope's Own Weight", Graduate Thesis, Seikei University, 1998 (In Japanese).
- (3) Ruze, J., "Antenna Tolerance Theory", Proc. IEEE, 54 April 1966, pp.633-640.